Effect of Pressure of Shock Wave Induced by Wire Explosion on Particle Size Distribution of Powdered Wire in Air

T. Koita, Y. Egawa, Y. Takaya, K. Oyama, S. Lim, T. Namihira, and C. Tokoro

Abstract This paper reports on the discussion of the effect of pressure behind the shock wave induced by the thin silver wire explosion on the particle size distributions generated in the electric explosion of wire (EEW) and the pulsed wire discharge (PWD) methods in the atmosphere. EEW and PWD were generated by the pulsed discharge with the charged voltage of 5.5 and 14 kV in the capacitor of 2.4 μF for the wire, respectively. The phenomena of EEW and PWD and the propagation shock waves emitted by the wire explosions in these methods were visualized optically. The visualized images indicated that the exploded wire with particles expanded behind the shock wave. The pressure of shock waves was calculated theoretically using the wave velocity analyzed with the visualized images. The maximum pressure of shock wave in PWD was higher than that in EEW. The range of particle size distribution generated by PWD was narrower than that by EEW. These results suggested that the finer powderzation with narrower-range particle distributions at PWD was generated by the higher pressure behind the shock wave.

Keywords Shock wave · Explosion · Pulsed discharge · Powderzation · Visualization

T. Koita (✉) · Y. Takaya · K. Oyama · C. Tokoro
Faculty of Science and Engineering, Waseda University, Tokyo, Japan
e-mail: koita@aoni.waseda.jp

C. Tokoro
e-mail: tokoro@waseda.jp

Y. Egawa
Graduate School of Creative Science and Engineering, Waseda University, Tokyo, Japan

Y. Takaya · C. Tokoro
Faculty of Engineering, The University of Tokyo, Tokyo, Japan

S. Lim
Faculty of Engineering, Nippon Bunri University, Oita, Japan

T. Namihira
Institute of Industrial Nanomaterials, Kumamoto University, Kumamoto, Japan

R. S. Myong and H. D. Kim (eds.), *Proceedings of the 34th International Symposium on Shock Waves, Volume 3: Applications 2*,
https://doi.org/10.1007/978-981-96-4775-0_40

1 Introduction

Many studies on the electric explosion of wire (EEW) and the pulsed wire discharge (PWD) methods in air for the powderization has been conducted [1–6]. EEW causes the wire evaporation due to the Joule heating caused by pulsed current. The wire is exploded with the volume expansion by the evaporation. The evaporated wire is rapidly cooled by the ambient air, resulting in the powderization with particles [1, 2]. PWD with the plasmaization appears in expanding particles caused by EEW in the air due to the arc discharge passing through the mixed medium with particles and air when the voltage higher than that occurring EEW is applied and the remained voltage in the discharge capacitor reaches the breakdown voltage of the medium. The plasmaization in PWD is called as the restrike in studies of pulsed discharge [5, 6]. The previous study suggested that, in the PWD, powdered particles of EEW are re-vaporized by the plasmaization at PWD, resulting in re-powdered [3]. The EEW method is traditionally used for ultrafine particle generation [1, 2].

Recently, the wire explosion with the restrike using PWD was applied to a novel electrical dismantling method for separating Cu and Ag busbars from a cell sheet from a waste photovoltaic panel has been studied experimentally [7, 8]. This study established a high-level recovery method, with a total average liberation of Cu and Ag particles of 94.3% and 77.5%, respectively; pulsed discharge in water at 13 kV and a capacitance of 40.8 μF were used. The PWD method is also suitable for reuse and recycling. The previous study visualized optically the generation of shock wave caused by EEW in the air with method [9]. This study indicates that the expanded wire with the evaporation in EEW eventually transformed into the powderzation in the pressure behind the shock wave caused by the explosion. Although the study was the generation of shock wave emitted by the wire explosion in EEW has performed, the phenomena of PWD and the shock wave induced by the explosion in PWD have not been much clarified.

The object of this study is to discuss the influence of shock wave pressures induced by wire explosions at EEW and PWD methods on the size distributions of powder particles recovered in these methods. The phenomena of wire explosions induced by EEW and PWD with the restrike and shock wave propagation emitted by these explosions were visualized optically. The pressure of shock waves was calculated theoretically using the wave velocity which was obtained by analyzing the visualized images. The effect of pressure behind the shock wave on the particle size distributions generated in EEW and PWD were discussed.

2 Experimental Method

The electric explosion of wire (EEW) and the pulsed wire discharge (PWD) were caused by the pulsed discharge in the air atmosphere. The test wire was an Ag wire of 99.99% purity with diameter of 50 μm and length of 150 mm (AG-401107, Nilaco

Corp., Japan). The length was same as that used in a previous study for recovering Ag particles from a cell sheet from a waste photovoltaic panel by PWD for Ag paste wires [7, 8].

Figure 1 shows a schematic diagram of the experimental set-up and circuit diagram of the pulsed discharge causing EEW and PWD methods. The EEW and PWD was performed in the wire between positive and negative electrodes by changing the charging voltage in the capacitor (V_c) to 14 kV with the DC power supply. Glass slides coated with a dispersing liquid were placed 100 mm below the wire, and particles generated by these methods were recovered in the liquid. The circuit consisted of charging and discharging sections. These circuits were changed manually by using a mechanical switch (E60-DT-80-1-15-BD, Ross Engineering). In the charging circuit, the capacitor was charged with a direct current (DC) power supply (152A, TDK Lambda) by changing the charging voltage of the supply. The charging voltage was changed by using a control unit. Three capacitors (FL40W804KWFAAA, Shizuki Electric Co., Inc.) were connected in parallel, and the total capacitance was 2.4 μF. A 1 kΩ resistor (TE1500B1K0J, TE Connectivity) was connected between the power supply and the parallel capacitors. When the switch was turned to the discharging section, the capacitor charge was rapidly released and the current flowed to the wire. As a result, a pulsed discharge was applied to the wire. The applied voltage and discharge current passing between two electrodes was measured by using a voltage probe (HV-P60A, Iwatsu) and a current transformer (Model110A, Pearson Electronics).

The shock wave propagation and wire powderization caused by EEW and PWD were optically visualized by the shadowgraph method. The visualized phenomena were recorded by a a high-speed video camera (HPV-X2, Shimadzu Corp.) with a resolution of 400 × 250 pixels. Figure 2 shows a schematic diagram of the optical arrangement and the recording system used for visualization. The arrangement consisted of a light source, two plane-convex lenses, and a high-speed video camera for recording the visualized phenomena. A pulsed-diode laser (Cavilux Smart, Cavitar) with a wavelength of 640 ± 10 nm and total power of 500 W was used as the light source. The pulse width of laser was set at 20 ns. An optical glass fiber was

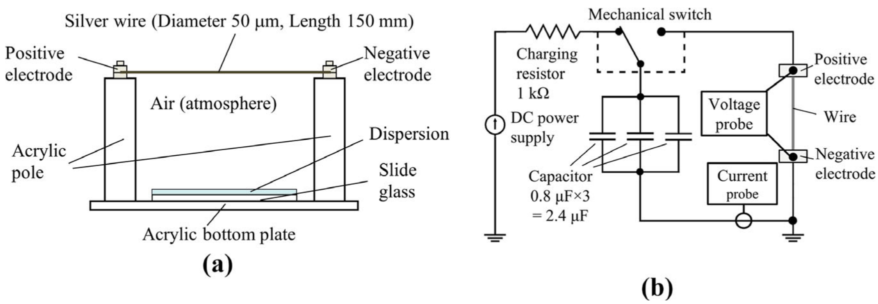

Fig. 1 Schematic diagram of **a** the experimental model of the pulsed discharge for the thin silver wire, **b** the circuit diagram of the discharge

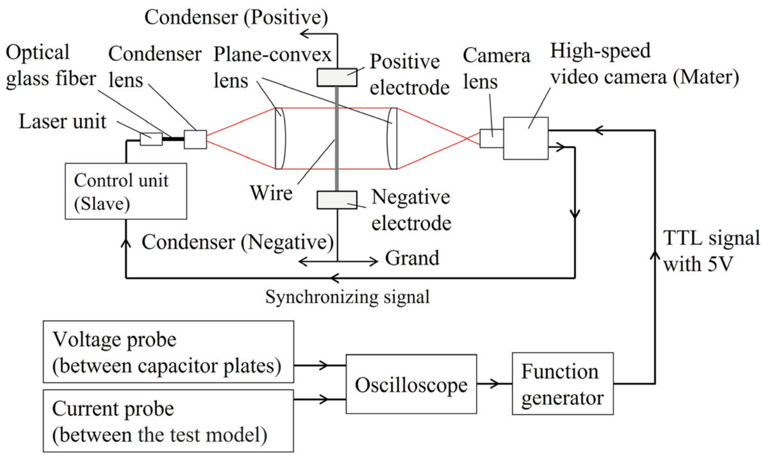

Fig. 2 Schematic diagram of the optical arrangement and the recording system for the visualization

installed in the laser unit, and a non-coherent and diffused laser was emitted because of the passage of the laser inside the fiber with reflection. The condenser lens was mounted on the tip of the fiber for irradiation of the plane-convex lens and generation of a parallel light in the sample wire. The camera lens, with a focal length of 300 mm and F-number of 3.5, was mounted on the camera. The recording conditions of the high-speed video camera were set at a frame rate of 5.00×10^6 frame/s, a frame interval of 200 ns, and an exposure time of 200 ns in the camera. In this shadowgraph, the recording exposure time was 20 ns, which was the pulse laser width. The start of light emission and recording of the high-speed video camera were synchronized with the voltage rise in the pulsed discharge.

3 Theoretical Analysis

The effects on the powdered particle size distribution causing in the pressure behind the shock wave (p_s) which was generated by EEW and PWD with the restrike, p_s was isentropically calculated by using the fundamental equations of continuity and momentum for a shock wave, Eqs. (1) and (2), and the equation of state for the shock wave shown in Eq. (3) [39].

$$\rho_0 U_s = \rho_s\left(U_s - U_p\right) \tag{1}$$

$$p_s - p_0 = \rho_0 U_s U_p \tag{2}$$

$$\frac{p_0}{\rho_0^{\gamma}} = \frac{p_s}{\rho_s^{\gamma}} \tag{3}$$

where p, ρ and U are the pressure, the density, and the velocity. The subscript 0 refers to the state of the ahead of shock wave front. The subscript s and p refer to the that of the shock wavefront and the gas particles behind the shock wave; γ is the specific heat ratio for the atmosphere, and γ of 1.4 was used. Combining Eqs. (1)–(3) gives the equation for the relationship between the velocity of shock wave and the pressure behind the wave as follows:

$$\left\{1-\left(\frac{p_s}{p_0}\right)^{-\frac{1}{\gamma}}\right\}\rho_0 U_s^2 - p_s + p_0 = 0 \tag{4}$$

The value of the shock wave velocity U_s, which was obtained by analyzing the visualized image, was substituted into Eq. (4), and the pressure p_s was calculated by using Newton's method in the equation.

To discuss the effect of deposited energy generating the wire explosion in EEW and PWD methods, E_{ew} and E_{wd}, on the shock wave pressure and diameters of particles caused by these methods, E_{ew} and E_{wd} were calculated by measured voltage V_{ew} and V_{wd}, current I_{ew} and I_{wd} at Δt in the current flow of the explosion as follows:

$$E_{\mathrm{ew}} = \sum V_{\mathrm{ew}} I_{\mathrm{ew}} \Delta t \tag{5}$$

$$E_{\mathrm{wd}} = \sum V_{\mathrm{wd}} I_{\mathrm{wd}} \Delta t \tag{6}$$

where V_{ew} and V_{wd} are measured voltages in the explosion at EEW and PWD, I_{ew} and I_{wd} are currents in these. Δt is the duration of time observed in the current waveforms during the explosion.

4 Results and Discussion

4.1 Phenomena of Wire Explosion Caused by Pulsed Discharge

The wire explosion in EEW and the explosion with the restrike in PWD occurred at V_{c} of 5.5 kV and 14 kV, respectively. Figures 3 and 4 show visualized images of the shock wave propagation induced by EEW and PWD and phenomena of wire restrike. Figure 5 presents the voltage and current waveforms at $V_{\mathrm{c}} = 5.5$, 14 kV of EEW and PWD.

When the wire exploded at $V_{\mathrm{c}} = 5.5$ kV, many particles with black shadows appeared in the atmosphere as shown in Fig. 3. The previous study of application of Ag wire explosion caused by the pulsed discharge on the separation of bonded resin plates was conducted in the same discharge circuit used in this study [10]. The study indicated numerically that the Ag wire temperature in the explosion at $V_{\mathrm{c}} = 5.5$ kV

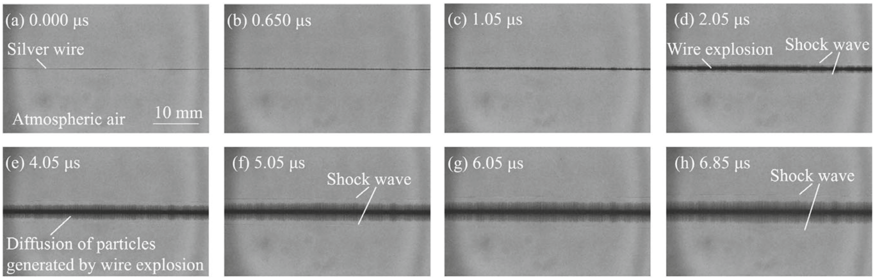

Fig. 3 Visualized images of wire explosion process and shock wave propagation induced by the electric explosion of wire (EEW) at $V_c = 5.5$ kV

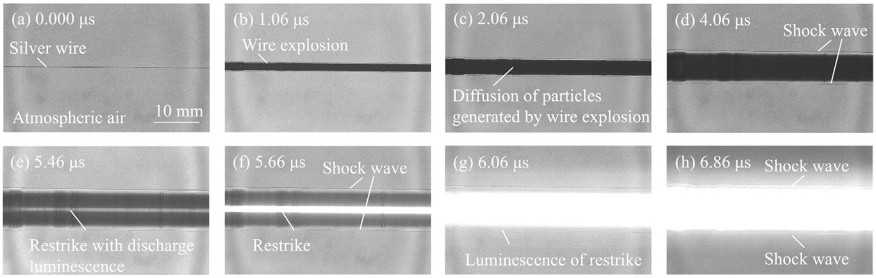

Fig. 4 Visualized images of wire explosion, restrike and shock wave propagation induced by the pulsed wire discharge (PWD) at $V_c = 14$ kV

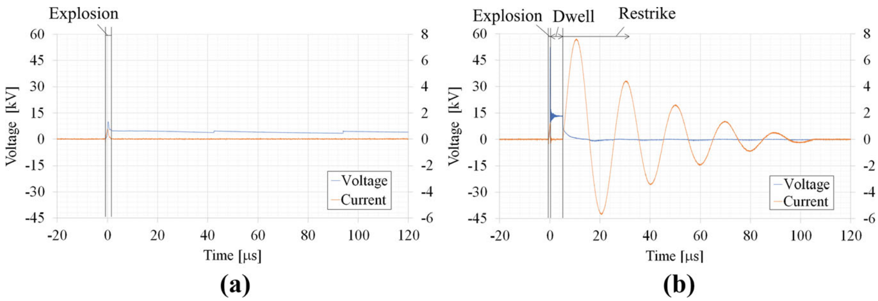

Fig. 5 Voltage and current waveforms between electrodes in the pulsed discharge where wire set **a** at $V_c = 5.5$ kV in EEW, **b** at $V_c = 14$ kV in PWD

was 2124 K, which is higher than the melting point of Ag and lower than the boiling point, resulting in volume expansion of the wire with liquefaction. The visualized particles could therefore be powdered wire particles formed by volume expansion without vaporization. The shock wave was observed in the front of the expanded particles in Fig. 3b–h. It was suitable to consider that the shock wave was generated by the compression of atmosphere surrounding the expanding wire with particles.

As seen in Fig. 4a, the maximum voltage V_{max} reached at 10.2 kV in time of 2.0 μs when the wire explosion of EEW appeared in V_c = 5.5 kV; the value of V_{max} was higher than V_c. The Ag wire melting and vaporization generated by pulsed discharge cause a sudden interruption of pulse current *i*. The voltage *Ldi*/*dt* with a circuit inductance *L* rose between two electrodes, result in the higher voltage of V_{max} than V_c. In PWD at V_c = 14 kV, Fig. 4d clearly showed that the explosion hardly appeared, and the shadow area increased. From the previous study, the wire temperature at t = 4.0 μs at V_c = 14 kV in PWD reached at 4405 K, which was higher than the boiling point of Ag [10]. This suggested that the wire was gasified by the current flow at the explosion in this study. The propagation of shock wave emitted by the wire explosion was observed in Fig. 4b–d. Figure 4e, f clearly indicates that restrike with discharge luminance appeared in the gas expansion of exploded wire. When the higher voltage than dielectric breakdown voltage of an expanding gasified wire remained in in the capacitor after the explosion, the redischarge, the restrike, occurred between the expanded gas due to the charge energy was released again [5, 6]. The luminance during expansion strengthened with time passage as shown in Fig. 4e–h. The voltage and current of explosion and restrike were observed in Fig. 5b. The time between the decrease in the current during the wire explosion and the subsequent increase in the current of restrike is called the dwell time [11]. The dwell appeared in Fig. 5b at V_c = 14 kV from the time of 5.46 μs. After the current has passed in the wire explosion, the voltage is sustained between the electrodes, and the current flows again in the gasified wire when the breakdown voltage of the medium consisting of atmospheric air containing Ag particles generated by the explosion was lower than the voltage.

4.2 Relationship Between the Deposited Energy of the Wire Explosion and the Shock Wave Pressure in EEW and PWD

Figure 6 shows the time histories of deposited energies of wire explosion, dwell and restrike at V_c = 5.5, 14 kV. The deposited energy generating of wire explosion in EEW and PWD, E_{ew} and E_{wd}, were obtained in Fig. 6 at the time Δ*t* when these phenomena observed in Fig. 5 of voltage and current waveforms. E_{ew} at V_c = 5.5 kV was 3.75 J. E_{ew} and E_{wd} induced by V_c = 14 kV were 6.93 J and 83.9 J, respectively.

Figure 7 presents the velocity of shock wave, U_s, analyzed the images of Figs. 3 and 4, and the pressure of the wave, p_s, calculated by the Eq. (4) using U_s in the wire explosion at V_c of 5.5 and 14 kV in EEW and PWD. The velocities of EEW and PWD reached maximally 753 and 1006 m/s at the time of 0.45 μs and 1.01 μs, respectively. When the current completely flows in the wire explosion at the time *t* of 5.0 μs, the velocities of shock waves were 559, 835 m/s. Maximum P_s of shock wave in the explosion at V_c = 14 kV reached 1006 kPa, and this was 1.58 times higher than that at V_c = 5.5 kV of 636 kPa. E_{ew} at 14 kV was 1.85 times larger than

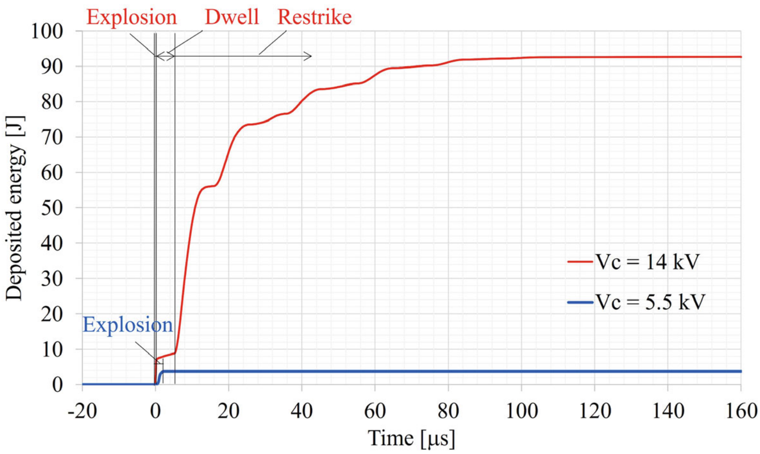

Fig. 6 Time histories of deposited energies of wire explosion, dwell and restrike at $V_c = 5.5$, 14 kV in EEW and PWD

that at 5.5 kV. These results indicated that the shock wave pressure induced by the wire explosion increased as the deposited energy of explosion increased.

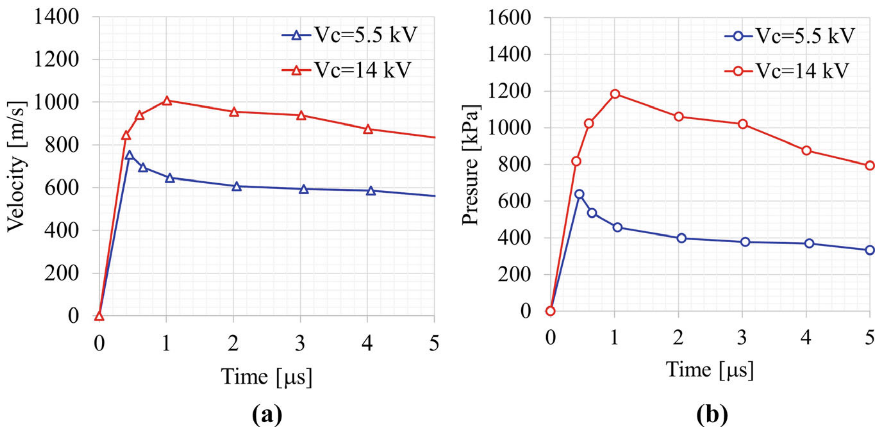

Fig. 7 Time histories of **a** analyzed velocity of shock wave, **b** calculated pressure of shock wave using the velocity at $V_c = 5.5$, 14 kV in EEW and PWD

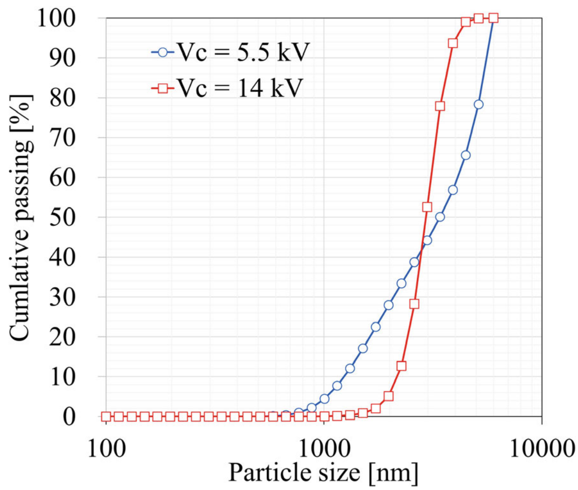

Fig. 8 Particle size distribution produced by V_c = 5.5, 14 kV in EEW and PWD

4.3 Discussion of Effect of Shock Wave Pressure in the Wire Explosion Caused by EEW and PWD on Wire Powderization

Figure 8 shows particle size distributions formed by the pulsed discharge at $V_c = 5.5$, 14 kV in EEW and PWD which were measured by a dynamic light scattering method. Figure 7 clearly indicated that these distributions were different. The distribution at $V_c = 5.5$ kV formed with the large particle size and the particle fraction near 6000 nm was majority. On the other hand, the distribution at V_c = 14 kV in PWD was more homogenous than that at V_c = 5.5 kV. The major grain size at V_c = 14 kV ranged from 1500 to 3000 nm, and finer powderzation occurred. The previous study [12] reported the median diameter produced by the wire explosion was smaller as the gas pressure increased.

From the results and the previous study, the pressure behind shock wave where the powder was produced by the wire explosion at V_c of 14 kV was higher than that at V_c of 5.5 kV, resulting in the finer powderzation.

5 Conclusions

The electric explosion of wire (EEW) and the pulsed wire discharge (PWD) occurred at the charged voltage of 5.5 and 14 kV in the capacitor with the capacitance of 2.4 μF.

The velocities of shock wave emitted in the wire explosion of EEW and PWD at these voltages which were obtained by analyzing the visualized images were 753 m/s and 1006 m/s, respectively. The maximum pressure of shock wave which was calculated theoretically with these velocities at the voltage of 5.5 and 14 kV reached

636 and 1006 kPa. The particle size distributions formed by the pulsed discharge at the voltage of 14 kV in PWD was narrower than that of 5.5 kV in EEW. It was possible to consider that the wire expanded without evaporation in EEW and the wire was gasified in the explosion at PWD. These results suggested that the finer powderzation with narrower-range particle distributions in PWD was generated by the higher pressure of powdered wire behind the shock wave in the evaporated wire.

References

1. Umakoshi, M., Yoshitomi, T., Kato, A.: Mater. J. Sci. **30**, 1240–1244 (1995)
2. Cho, C., Choi, Y.W., Kang, C., Lee, G.W.: Appl. Phys. Lett. **91**(14), 2–5 (2007)
3. Jiang, W., Yatsui, K.: IEEE Trans. Plasma Sci. **26**(5), 1498–1501 (1998)
4. Suzuki, T., Keawchai, K., Jiang, W., Yatsui, K.: Jpn. J. Appl. Phys. **40**, 1073–1075 (2001)
5. Vlastós, A.E.: J. Appl. Phys. **39**(7), 3081–3087 (1968)
6. Vlastós, A.E.: J. Appl. Phys. **43**(4), 1985–1987 (1972)
7. Tokoro, C., Lim, S., Sawamura, Y., Kondo, M., Mochidzuki, K., Koita, T., Namihira, T., Kikuchi, Y.: Int. J. Autom. Technol. **14**(6), 966–974 (2020)
8. Lim, S., Imaizumi, Y., Mochidzuki, K., Koita, T., Namihira, T., Tokoro, C.: IEEE Trans. Plasma Sci. **49**(9), 2857–2865 (2021)
9. Qian, D., Liu, Z., Li, L., Zou, X., Wang, X.: IEEE Access **8**, 85968–85972 (2020)
10. Egawa, Y., Koita, T., Lim, S., Namihira, T., Tokoro, C.: IEEE Trans. Dielectr. Electr. Insul. **30**(1), 449–457 (2022)
11. Vlastós, A.E.: J. Appl. Phys. **44**(5), 2193–2196 (1973)
12. Sarathi, R., Sindhu, T.K., Chakravarthy, S.R.: Mater. Charact. **58**(2), 148–155 (2007)